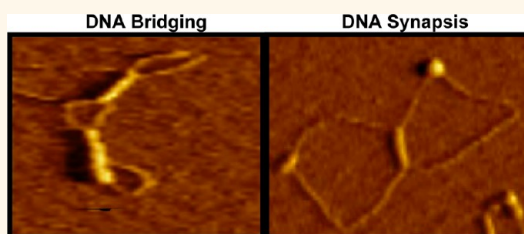


# Single-Molecule DNA Analysis Reveals That Yeast Hop1 Protein Promotes DNA Folding and Synapsis: Implications for Condensation of Meiotic Chromosomes

Krishnendu Khan,<sup>†</sup> Usha Karthikeyan,<sup>†</sup> You Li,<sup>‡</sup> Jie Yan,<sup>‡</sup> and K. Muniyappa<sup>†,\*</sup>

<sup>†</sup>Department of Biochemistry, Indian Institute of Science, Bangalore 560012, India and <sup>‡</sup>Department of Physics & Mechanobiology Institute, National University of Singapore, Singapore 117542

**ABSTRACT** During meiosis, long-range interaction between homologous chromosomes is thought to be crucial for homology recognition, exchange of DNA strands, and production of normal haploid gametes. However, little is known about the identity of the proteins involved and the actual molecular mechanism(s) by which chromosomes recognize and recombine with their appropriate homologous partners. Single-molecule analyses have the potential to provide insights into our understanding of this fascinating and long-standing question. Using atomic force microscopy and magnetic tweezers techniques, we discovered that Hop1 protein, a key structural component of *Saccharomyces cerevisiae* synaptonemal complex, exhibits the ability to bridge noncontiguous DNA segments into intramolecular stem-loop structures in which the DNA segments appear to be fully synapsed within the filamentous protein stems. Additional evidence suggests that Hop1 folds DNA into rigid protein–DNA filaments and higher-order nucleoprotein structures. Importantly, Hop1 promotes robust intra- and intermolecular synapsis between double-stranded DNA molecules, suggesting that juxtaposition of DNA sequences may assist in strand exchange between homologues by recombination-associated proteins. Finally, the evidence from ensemble experiments is consistent with the notion that Hop1 causes rigidification of DNA molecules. These results provide the first direct evidence for long-range protein-mediated DNA–DNA synapsis, independent of crossover recombination, which is presumed to occur during meiotic recombination.



**KEYWORDS:** meiosis · Hop1 protein · DNA bridging · DNA condensation · long-range DNA interactions · Holliday junction

The pairing of homologous chromosomes in meiosis, assembly of the synaptonemal complex (SC), and crossover recombination are all crucial for the formation of chiasmata. SC consists of two dense lateral elements (LE), each one associated with a pair of chromatids, a less dense central element, which are joined by numerous transverse filaments.<sup>1–3</sup> From yeast to humans, it is known that defects in the formation of SC leads to high rates of aneuploidy in the mature gametes.<sup>4</sup> Characterization of the full complement of SC proteins and functional significance of these proteins remain important areas of investigation. However, only a few components of LE have been described in yeast, mammals, plants, and *Caenorhabditis*

*elegans*. In *Saccharomyces cerevisiae*, the known SC components include Hop1, Red1, Zip1, Zip2, Zip3, and Mek1.<sup>5–8</sup> Hop1 and Red1 proteins are structural components of LE, which colocalize to the axial cores of meiotic chromosomes and are required for homologous chromosome synapsis as well as chiasma formation.<sup>5,6,9,10</sup> Mutational analyses in *S. cerevisiae* have shown that sister chromatid cohesion is required for proper chromosome condensation, including the formation of axial elements, SC assembly, and recombination.<sup>11</sup> Consistent with these findings, homologue alignment is impaired in hop1 red1 strains and associations between homologues are less stable.<sup>12,13</sup> The red1 mutants fail to make any discernible axial elements or SC structures but exhibit

\* Address correspondence to kmcb@biochem.iisc.ernet.in.

Received for review August 21, 2012 and accepted November 4, 2012.

Published online November 05, 2012  
10.1021/nn3038258

© 2012 American Chemical Society

normal chromosome condensation, while *hop1* mutants form long fragments of axial elements but without any SCs, are defective in chromosome condensation, and produce inviable spores.<sup>6,13,14</sup> The functional homologues of Hop1 protein exist across species including *Arabidopsis thaliana*,<sup>15</sup> *C. elegans*,<sup>16</sup> and mammals,<sup>17</sup> indicating that *HOP1* function is conserved throughout evolution. Here, we will use the terms “pairing” to describe all aspects of association between homologous DNA molecules and “synapsis” to describe the association between DNA sequences promoted by SC-associated proteins.

Previous studies have suggested that *S. cerevisiae* Hop1 protein plays an important role in meiosis by virtue of its ability to monitor the progression of recombination intermediates through meiotic prophase.<sup>18–20</sup> Here, we reveal that Hop1 protein organizes DNA into at least three major distinct DNA conformations: (i) bridging of noncontiguous segments of DNA to form stem-loop structures; (ii) intra- and intermolecular long-range synapsis between double-stranded DNA molecules; (iii) folding of DNA into rigid nucleoprotein filaments and compact DNA structures that block the nuclease's access to the DNA backbone. These results provide novel insights into Hop1 protein function in meiotic chromosome condensation and long-range synapsis between double-stranded DNA molecules and recombination.

## RESULTS

**Hop1 Protein Bridges Noncontiguous DNA Segments into Stem-Loop Structures.** To gain insights into the mechanism of long-range interactions between homologous chromosomes during meiosis, we have used atomic force microscopy (AFM) to directly visualize the spatial pattern of Hop1 protein–DNA interactions at the single-molecule level. For these studies, we incubated Hop1 with relaxed circular duplex DNA under optimal binding conditions.<sup>20</sup> The AFM images of Hop1–DNA complexes were acquired under ambient conditions in air. Figure 1A shows an AFM image of relaxed circular duplex DNA. Qualitative examination of a large number of molecules from reactions containing Hop1 (100 nM) and circular duplex DNA (5 ng) indicated that Hop1 promotes the formation of structurally distinct higher-order nucleoprotein complexes. Consistent with this notion, a representative image shown in Figure 1B reveals the coexistence of three distinct types of Hop1–DNA complexes, thus implying that Hop1 has the ability to fold DNA into three different types of higher-order structures: first, cooperative binding of Hop1 to circular duplex DNA led to the formation of rigid, rod-like filaments (yellow arrows, Figure 1B). The second type of binding involves bridging between noncontiguous DNA segments to form intramolecular stem-loop structures in which the duplex DNA segments appear to be fully synapsed within the nucleoprotein filament stems (white arrows, Figure 1B–H). A few

randomly selected AFM images shown in Figure 1C–H confirm that Hop1 promoted bridging between circular duplex DNA molecules. Subsequently, cooperative binding of Hop1 extends these bridges into rigid, rod-like structures. Indeed, as shown in Figure 1B–H (yellow arrows), full-length as well as regions of circular duplex DNA has condensed into rod-like structures. The contour lengths of naked circular duplex DNA, compared to circular duplex DNA complexed with Hop1, revealed a 4-fold reduction, from 1200 to 300 nm, indicating that binding of Hop1 induces DNA condensation and the formation of higher-order structures. A third type of Hop1–DNA complex often observed to exhibit significant compaction due to a high degree of DNA condensation appears as discrete “globules” (green arrow, Figure 1B,D,F,G) and short and long rod structures (yellow arrow, Figure 1B–H). We found that certain regions of DNA–Hop1 filaments have a greater height and width than others (Figure 1E,G,H). Some of these globules are so large that they may arise due to multiple levels of folding of Hop1–DNA filaments and may be directly responsible for the formation of large supramolecular structures. Although the functional significance of these globules is unknown, it is possible that they might be important at a number of steps that lead up to progressive condensation and coiling of chromosome fibers during meiosis.<sup>1–3</sup> Similar results were obtained in experiments performed with a variety of other conditions including various buffers, ion concentration range of 10 to 50 mM, and pH between 6.5 to 8 (data not shown).

In order to understand the architecture of Hop1-promoted DNA–DNA bridge and intermolecular synaptic structures, we determined the widths of the bridge formed between two noncontiguous segments of DNA (Figure 2A), the intermolecular synaptic structure formed between circular duplex DNA (Figure 2B), as well as linear duplex DNA molecules (Figure 2C). Figure 2D provides information on the widths of naked DNA as well as those of the Hop1–DNA filament, bridge, and synaptic structures. This analysis has revealed that there is sizable similarity in the widths of Hop1–DNA filament and DNA–DNA bridges as well as synaptic structures, indicating that the bridges and synaptic structures are formed between a DNA–Hop1 filament and segments of naked DNA and not between two DNA–Hop1 filaments (Figure 2E). Although the *in vivo* significance of these interactions is unknown, these results are consistent with the notion that Hop1 might be able to facilitate long-range interactions between homologous chromosomes during meiosis.

**Hop1 Protein Promotes Intra- and Intermolecular Synapsis between DNA Molecules.** We next investigated the ability of Hop1 protein to promote DNA synapsis between linear and circular double-stranded DNA molecules. Binding reactions were performed with circular or linear double-stranded DNA with lower concentrations

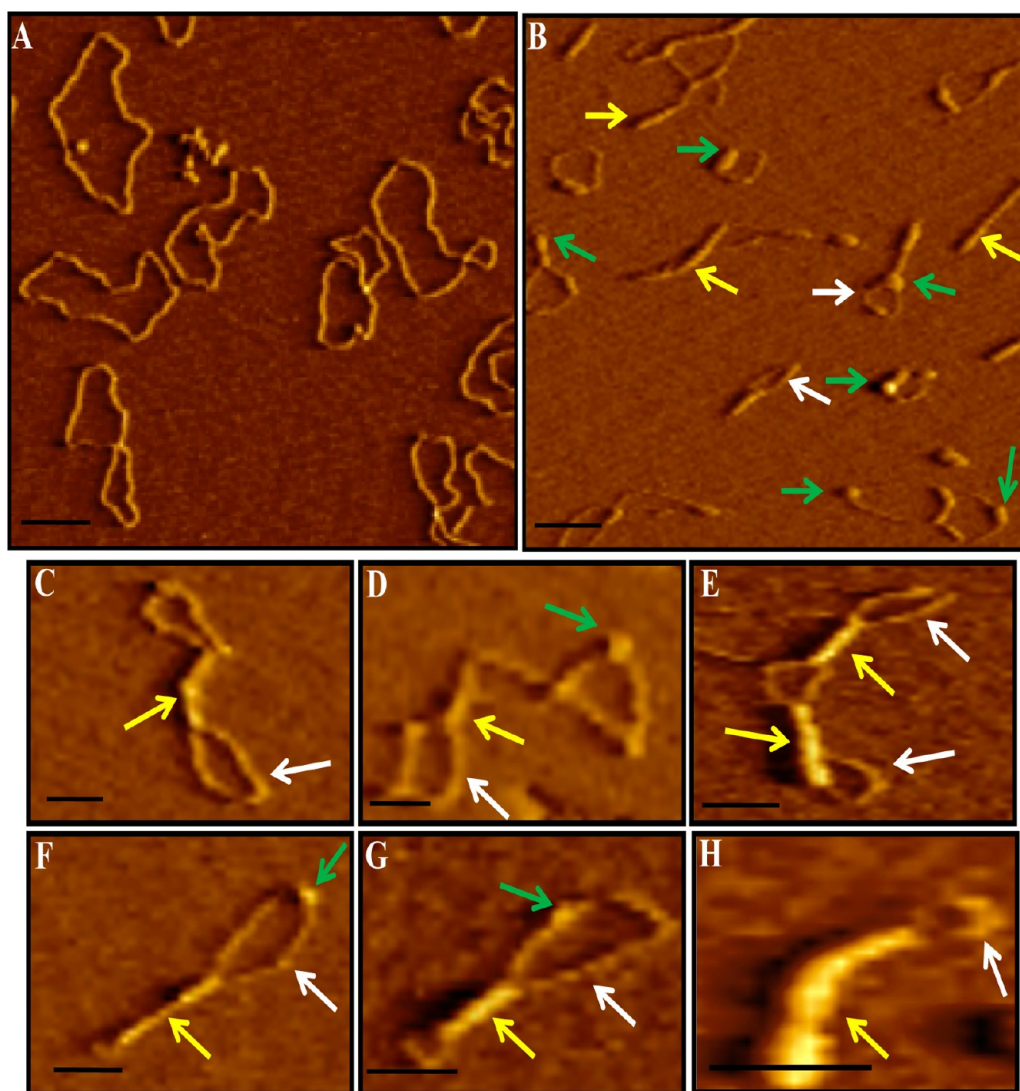


**Figure 1.** Hop1 protein promotes bridging of noncontiguous DNA segments into stem-loop structures. Reaction mixtures contained 5 ng of circular pNB10 plasmid DNA and 100 nM Hop1 protein. Five microliter aliquots were spotted on fresh mica and visualized as described in Methods. (A) Image frame of pNB10 circular DNA in the absence of Hop1 and (B) in the presence of Hop1 protein. (C–H) Randomly selected AFM images of Hop1–DNA nucleoprotein filaments. In the presence of Hop1 protein, frequently observed structures include stiff rod-like structures due to bridging and condensation of DNA (yellow arrow), loop structures (white arrow), and higher-order nucleoprotein structures, which appear as globules to smaller rods (green arrow). The scale bars represent 200 nm (A,B) and 100 nm (C–H).

of Hop1 protein to reduce the multimerization of DNA molecules. Like circular double-stranded DNA (Figure 1A), the linear duplex DNA molecule is well spread on the mica surface (Figure 3A). Figure 3B–I shows that Hop1 protein was able to promote intra- and intermolecular synapsis between circular or linear DNA molecules. Furthermore, the synapsis promoted by Hop1 between two linear DNA molecules *in trans* shows a typical X-like synaptic configuration. The two linear DNA molecules are usually joined at only one place along their length, although often joining at multiple places was also observed (Figure 3B–F yellow arrows). Notably, we found that Hop1 protein was able to promote synapsis between noncontiguous segments of linear DNA. These results suggest that the formation of intramolecular synaptic structures is

independent of sequence homology. The AFM images also show that the Hop1 protein generated globules at the synaptic joint and elsewhere in the molecule (Figure 3B–F, green arrows). The linear DNA seems to be condensed as evidenced by shortening of the contour length, suggesting that condensation is not constrained to the topologically closed circular DNA. The width analysis indicated that the DNA duplexes in the *trans*-synaptic complex are arranged in a side-by-side orientation.

#### Hop1 Protein Folds DNA into Stable Nucleoprotein Structures.

DNA-distorting proteins can affect the force–response of a single DNA tether, which allows us to investigate DNA binding of a protein at a single-DNA resolution.<sup>21,22</sup> To investigate Hop1 protein-induced DNA folding and condensation, we conducted experiments



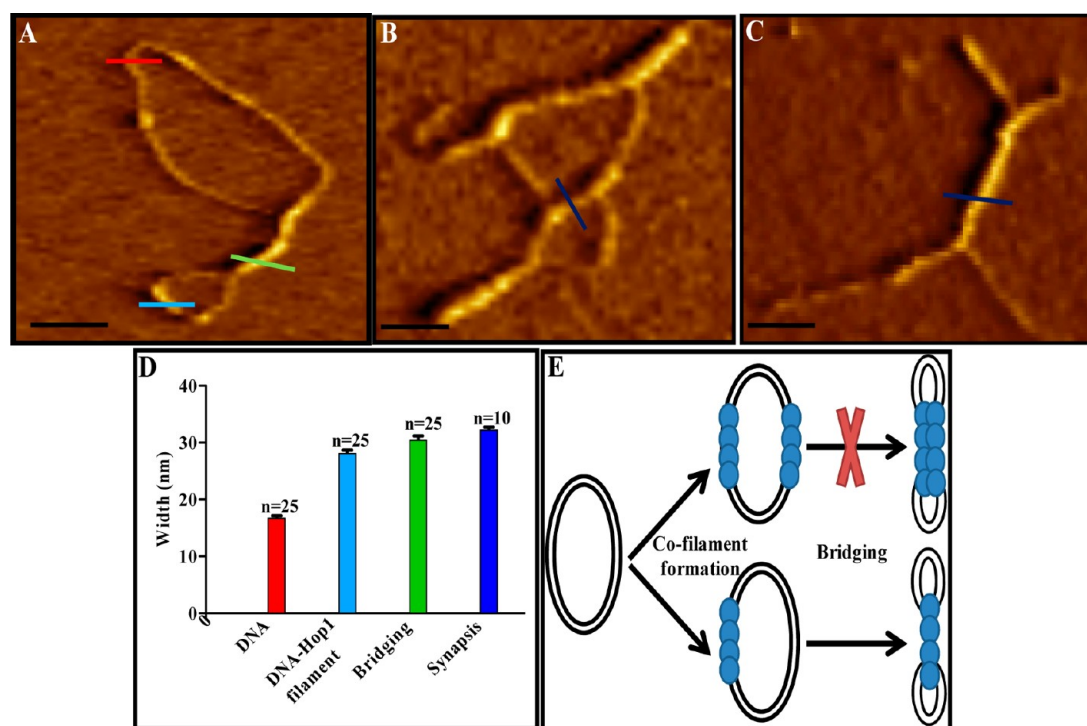


**Figure 2.** AFM imaging shows that Hop1 protein promotes DNA bridging between the DNA-bound Hop1 filament and the free DNA segment rather than between two DNA–Hop1 filaments. (A) Image of DNA bridging; (B) image of DNA–DNA synapsis between circular DNA molecules; (C) image of DNA–DNA synapsis between linear DNA molecules. (D) Histograms showing the width of naked DNA, Hop1 nucleoprotein filament, and DNA bridge and synapsis promoted by Hop1. (E) Hypothetical models of Hop1-promoted DNA bridging and DNA–DNA synapsis. The color bars in the AFM image frames indicate the areas used for quantification. In all images, the scale bars represent 100 nm.

with a transverse magnetic tweezers setup.<sup>23,24</sup> The experimental setup includes one end of biotin-labeled phage  $\lambda$ -DNA tethered to a coverslip *via* streptavidin, and the other is coupled to a paramagnetic bead. We measured the length of the Hop1–DNA complex under different tensile forces and compared it to the force–extension curve of naked DNA. We first applied a high force ( $\sim 10$  pN) to prevent DNA folding during addition of the protein solution. Then, we reduced the force successively to  $\sim 0.03$  pN, giving us the forward curve. Afterward, we increased the force successively back to high force, giving us the reverse curve. At each force, the DNA was held for 50–70 s and the extension was averaged from the last 10 s of data. Overlapping forward and reverse curves mean that the DNA–protein complex is at a steady state over the time scale, whereas non-overlapping curves (*i.e.*, hysteresis) hint to protein-induced DNA folding occurring over the time scale. Figure 4A shows that Hop1-induced DNA folding starts at 100 pM, as evidenced by the apparent hysteresis. In the presence of 500 pM Hop1 protein, DNA starts to fold at a larger force of  $\sim 6$  pN. At  $\sim 0.25$  pN, DNA folds quickly and the extension becomes less than  $2 \mu\text{m}$ , which is the minimal extension ( $\sim 2 \mu\text{m}$ ) that can be measured by our instrument. The folding at this force is indicated by a downward arrow in the figure.

Notably, our data suggest that Hop1 protein-induced DNA folding is highly stable. For example, at 100 pM

Hop1 protein, DNA extension was still below the values for naked DNA extension at 10 pN in the reverse curve, suggesting that the folded DNA at lower force value could not be unfolded at  $\sim 10$  pN over the time scale. In the presence of 500 pM Hop1 protein, the highly folded DNA could not be opened at even higher force ( $>20$  pN) applied for a long period of time ( $>30$  min). These results provide compelling evidence that Hop1 protein binds to DNA with high binding affinity (sub-nanomolar  $K_d$ ), which abets DNA folding into a highly stable nucleoprotein structure. These results further support the idea that Hop1 protein induces folding of double-stranded DNA and forms a tight protein–DNA complex to facilitate the formation of higher-order nucleoprotein structures.

Previous studies have shown that Hop1 protein contains a zinc-finger motif, which is essential for its *in vitro* and *in vivo* activities.<sup>25</sup> It was therefore of interest to determine the effect of  $\text{ZnCl}_2$  on Hop1-mediated DNA folding. In these experiments, we omitted  $\text{ZnCl}_2$  from the reaction buffer. In addition, Hop1-bound zinc ions were depleted from the protein by the addition of ethylenediaminetetraacetate (EDTA). As shown in Figure 4B, zinc-depleted Hop1 was unable to fold DNA at sub-nanomolar concentrations. However, zinc-depleted Hop1 protein was able to fold DNA at a concentration ( $\sim 11.6$  nM) that is 23-fold higher than the concentration needed to fold DNA in the presence of 0.1 mM  $\text{ZnCl}_2$  (Figure 4A).

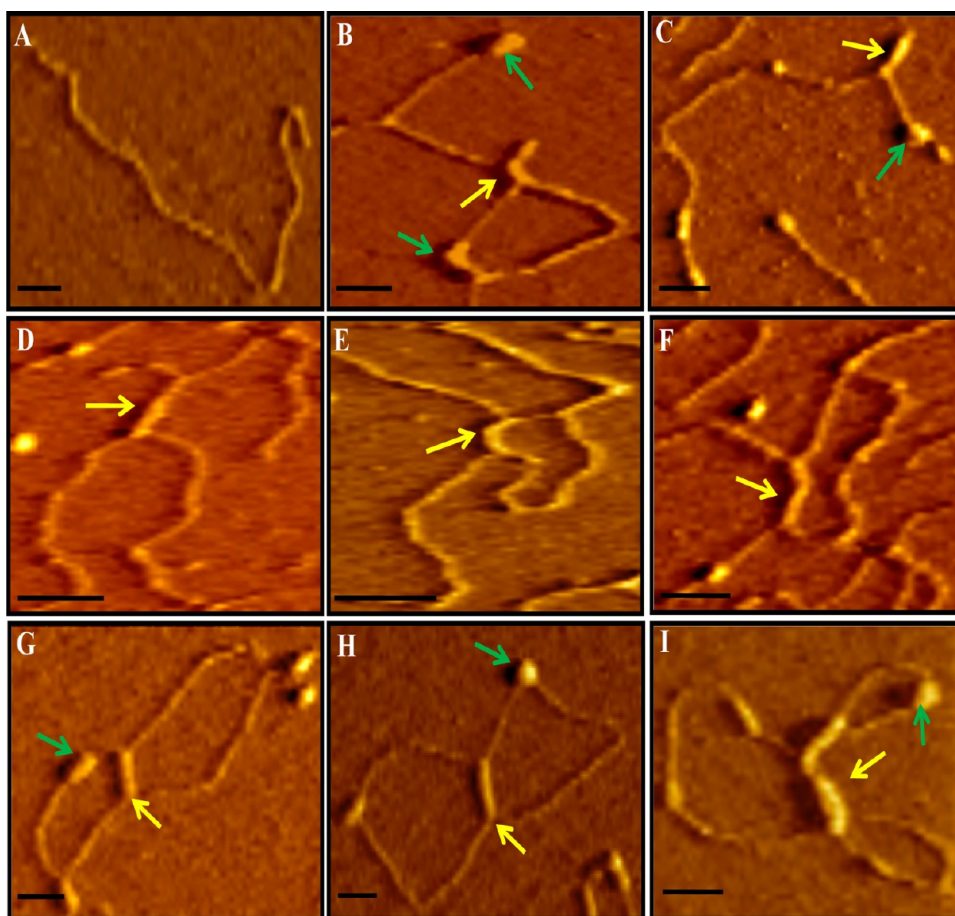


**Figure 3.** Hop1 protein promotes inter- and intramolecular synthesis between double-stranded DNA molecules. Reactions were performed as described in the legend to Figure 1, in the absence or presence of 100 nM Hop1. (A) AFM image of pET21a linear plasmid DNA alone. (B–I) Randomly selected AFM snapshots of intra- (B,C) and intermolecular (D–F) synthesis of linear double-stranded DNA. (G–I) Intermolecular synthesis of circular plasmid DNA. In all images, the scale bars indicate 100 nm.

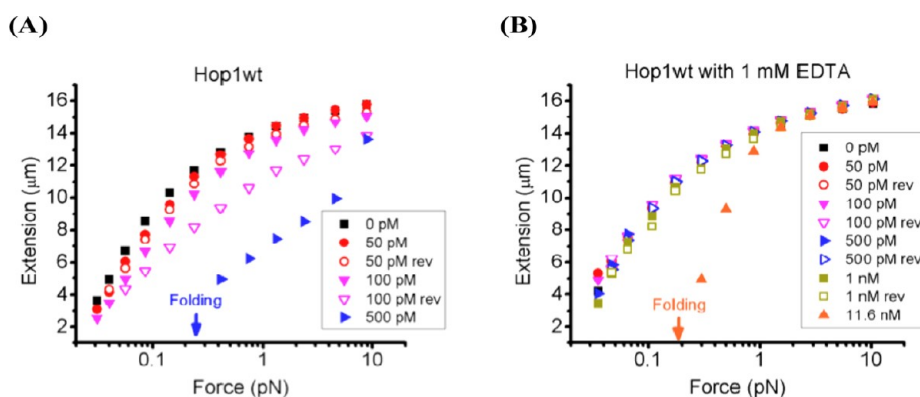


**Figure 4.** Hop1 protein promotes DNA folding and formation of rigid DNA–Hop1 protein filaments. Binding reactions were performed in a buffer containing 20 mM Tris-HCl (pH 7.5), 50 mM NaCl, 0.1 mM ZnCl<sub>2</sub> (where indicated), and indicated concentrations of Hop1 protein at 30 °C. (A) Black squares indicate extension of  $\lambda$ -DNA in the absence of Hop1. Filled symbols are the extension of the same DNA in the presence of Hop1 when force was gradually dropped. At each force, the extension was recorded for 50–70 s. Data recorded in the last 10 s were used to obtain the final extension and plotted in the figure. The open symbols show the extension of the same DNA (after being folded) when the force was increased (indicated by rev). At each force, the extension was recorded for 60 s (except for 500 pM Hop1, the unfolding data were recorded for 30 min). (B) ZnCl<sub>2</sub> plays an important role in folding of DNA by the Hop1 protein.

**Hop1 Protein Binding Abrogates Accessibility of DNA to Nucleases and Circularization of Linear DNA.** The AFM and magnetic tweezers data have provided compelling evidence that Hop1 promotes DNA rigidification and

condensation as well as the formation of stem-loop structures. Since DNA looping is conceptually similar to that of covalent joining of the ends of linear DNA to generate closed circular DNA molecules,<sup>26</sup> we reasoned

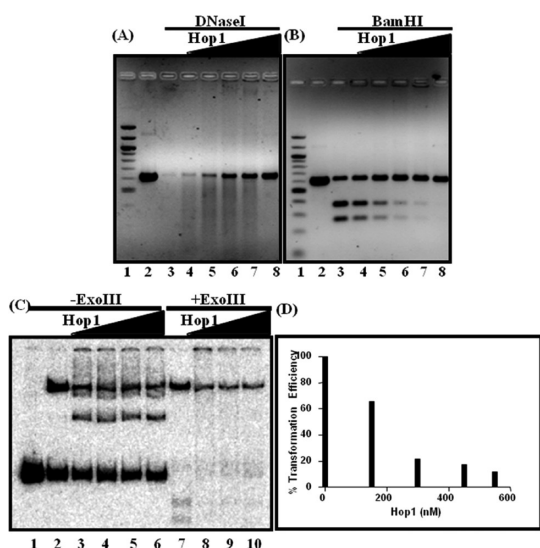


**Figure 5.** Hop1–DNA filaments abrogate the endonuclease activity and DNA circularization. The results in panels A and B show that Hop1 inhibits cleavage of linear double-stranded DNA by DNase I and *Bam*HI, respectively. (A) Lane 1, kb ladder DNA markers; lane 2, DNA in the absence of DNase I; lane 3, in the presence of DNase I; and lanes 4–8, Hop1 protein at 0.5, 1, 1.5, 2, and 2.5  $\mu$ M, respectively, and then incubated with DNase I. (B) Lane 1, kb ladder DNA markers; lanes 2, DNA in the absence of *Bam*HI; lane 3, in the presence of *Bam*HI; and lanes 4–8, in the presence of Hop1 at 0.5, 1, 1.5, 2, and 2.5  $\mu$ M, respectively, and then treated with *Bam*HI. Closed arrow on top of the gels in panels A and B indicates increasing concentrations of Hop1 protein. (C) Hop1 protein abrogates circularization of linear DNA by ligase. Lane 1, linear double-stranded DNA alone; lane 2 and 7, linear DNA in the presence of DNA ligase; lanes 3–6 (150, 300, 450, and 550 nM) and 8–10 (300, 450, and 550 nM), contained Hop1 as indicated, followed by incubation with phage T4 DNA ligase; lanes 7–10, the ligation products treated with Exo III. (D) Hop1 protein suppresses the transformation efficiency of plasmid DNA in *E. coli*. Percentage transformation efficiency of linear pUC19 plasmid DNA was performed in the absence or presence of 150, 300, 450, and 550 nM Hop1 protein, respectively. Histograms show the transformation efficiency as percentage calculated against the number of colony-forming units obtained with an equivalent amount of pUC19 plasmid DNA in the absence of Hop1 protein.

that Hop1–DNA loops may interfere with DNA cyclization by ligase, and filaments could reduce or block accessibility of DNA to endonucleases.

To test this premise, we first examined the effect of Hop1 filament formation on DNase I cleavage, which requires accessibility to  $\sim$ 6 bp of exposed DNA. The reactions were performed as described in Methods. Control experiments showed that DNA was completely digested by DNase I in the absence of Hop1 protein (Figure 5A, lane 3). On the other hand, incubation with increasing concentrations of Hop1 protein prior to DNase I treatment led to an increase in the protection of DNA (Figure 5A, lanes 4–8). We sought to confirm this result *via* an alternative DNA protection assay using *Bam*HI. Control reactions showed that *Bam*HI cleaved the DNA fragment into two faster migrating DNA species (Figure 5B, lane 3). Incubation with Hop1

protein prior to *Bam*HI treatment resulted in full protection from DNA cleavage (Figure 5B, lanes 4–8).

We next sought to investigate the effect of Hop1 nucleoprotein filament formation on DNA cyclization by ligase. The ligation products were examined for the presence of closed circular DNA. In the presence of Hop1 protein, we observed an intermediate band, presumably a linear dimer, and a slower migrating minicircle DNA (Figure 5C, compare lane 2 with lanes 3–6). This possibility was assessed by Exo III digestion of reaction products. Exo III treatment led to the removal of the linear dimer and slightly decreased the amount of DNA minicircles (Figure 5C, lanes 7–10), indicating that a portion of DNA minicircles may exist as nicked open circular form. Furthermore, Hop1 protein also inhibited DNA circularization, as evident from results of the transformation assay where linear pUC19 DNA was incubated with varying amounts Hop1 protein and T4 DNA ligase followed by transformation of *E. coli* DH5 $\alpha$  cells (Figure 5D).

## DISCUSSION

In this study, we have sought to understand the molecular mechanism(s) underlying long-range recognition between homologous chromosomes during meiosis. We show that Hop1 protein bridges and folds DNA and mediates long-range synapsis between double-stranded DNA molecules, thereby disclosing an important and previously unknown function of Hop1 protein. Additional evidence shows that Hop1 induces DNA condensation, and that it promotes both inter- and intramolecular synapsis, in a sequence-independent manner. Moreover, we show that Hop1-induced DNA folding is highly stable, and that the rigid Hop1 nucleoprotein filament protects DNA from nucleases and inhibits circularization of DNA molecules.

How do homologous chromosomes recognize one another in the recombination independent pairing phase? In 1933, B. McClintock proposed that “*there is a tendency for chromosomes to associate 2-by-2 in the prophase of meiosis*”.<sup>27</sup> During meiosis, sister chromatid cohesion is essential for interhomologue recombination, but the relationship between the two processes is poorly understood. It has been thought that the SC components play important roles in chromosome condensation, pairing, and recombination.<sup>1,2</sup> In fact, limited evidence exists suggesting that the central region of SC exhibits the tendency to synapse pairs of chromosomal axes until maximal synapsis is achieved.<sup>1–3,14</sup> Although nonhomologous synapsis has been observed in several yeast meiotic mutants that undergo delayed synapsis,<sup>2,28</sup> the relationship between nonhomologous synapsis and pairing of meiotic chromosomes remains poorly understood. Several lines of evidence suggest that homologous recombination during meiosis involves a complex series of biochemical reactions. In contrast to our current understanding of DNA strand



exchange processes promoted by the RecA/Rad51/Dmc1 family of proteins,<sup>29</sup> the molecular basis of recombination-independent synapsis of homologues remains a mystery. However, theoretical models posit that protein-mediated nonhomologous synapsis during meiosis plays important roles in the recognition of homologous DNA sequences, which are distant in three-dimensional space as well as among an overwhelming excess of heterologous DNA.<sup>28,30</sup>

We showed previously that Hop1 was able to promote interstitial pairing of duplex DNA molecules *via* the formation of G-quartets.<sup>31,32</sup> However, the functional relevance of interstitial pairing between two short duplex DNA molecules to long-range DNA interactions has remained elusive. In this work, we provide direct evidence in support of the ability of Hop1 to promote long-range DNA interactions, bridging, and condensation. To this end, single-molecule experiments indicate that Hop1 acts cooperatively to promote DNA bridging and folding, thus leading to the formation of higher-order nucleoprotein structures. Consistent with this notion, abrogation of DNA cyclization suggests that Hop1 protein binding affects DNA persistence length. At the ultrastructural level, SC has been defined as a zipper-like structure that forms between homologues along their entire length, with an array of radial loops of chromatin fibers anchored to the lateral elements in a manner analogous to lampbrush chromosomes.<sup>1–3</sup> Since the Hop1 protein is a key structural component of LEs, it is possible that the intramolecular loops formed by the Hop1 protein might correspond to radial chromatin loops. Furthermore, DNA bridging and loop formation could

potentially play important roles, not only in synapsis but also in other aspects of meiotic prophase. For example, double-strand breaks and recombining sequences map to chromatin loops in yeast.<sup>33–35</sup> We speculate that the ability of Hop1 protein to promote long-range DNA interactions, resulting in a compartmentalized chromosome conformation, might help recombination-associated proteins in their genome-wide search for homologous sequences.

Genetic and biochemical studies during the past three decades have unravelled many of the mechanistic aspects of DNA strand exchange between homologous sequences.<sup>29</sup> By contrast, the mechanism by which the interacting DNA molecule finds its match in a vast milieu of nonhomologous sequences is largely unknown. Specifically, the question arises as to how the two homologous needles find each other in the genomic haystack. Indeed, it has been surmised that pairing of homologues in the absence of recombination is an initial coarse recognition step, followed by double-strand breakage and subsequent recombination.<sup>35–37</sup> From a biological perspective, our study supports the notion that the Hop1 protein as a mediator of long-range synapsis *via* DNA bridging and condensation may facilitate strand exchange proteins to catalyze DNA strand exchange between homologous sequences. Furthermore, the mechanisms underlying meiotic chromosome condensation and homologue synapsis are incompletely defined and probably involve several mechanisms. Our study provides a framework for understanding the roles of SC components in the regulation of meiotic chromosome recognition, synapsis, and recombination.

## METHODS

**Biochemicals, Proteins, and DNA.** Fine chemicals were purchased from GE Healthcare Biosciences and Sigma Chemical Company (St. Louis, MO, USA). Restriction endonucleases were obtained from New England Biolabs, USA. T4 DNA ligase and T4 polynucleotide kinase were purchased from Fermentas (USA). Linear duplex DNA was labeled at the 5'-end by using [ $\gamma$ -<sup>32</sup>P]ATP (Bhabha Atomic Research Centre, Mumbai, India) and T4 polynucleotide kinase. pUC19, pNB10, and pET21a plasmid DNA were isolated from cultures of *E. coli* DH5 $\alpha$  strain using a Qiagen maxiprep kit and were resuspended in water. Negatively superhelical (form I) plasmid DNA was treated with wheat germ topoisomerase I or linearized using appropriate restriction endonucleases as specified by the manufacturer (New England Biolabs) and purified using Qiagen gel extraction kit. *S. cerevisiae* Hop1 protein was purified as previously described.<sup>26,38</sup>

**Atomic Force Microscopy.** *S. cerevisiae* Hop1 was incubated with the indicated amounts of DNA in buffer [20 mM Tris-HCl (pH 7.5), 0.1 mM ZnCl<sub>2</sub>, and 2 mM MgCl<sub>2</sub>] at 30 °C for 30 min. Aliquots (5  $\mu$ L) of the reaction mixtures were deposited onto freshly cleaved mica (Spruce Pine Mica Company, Spruce Pine, NC, USA) and allowed to bind for 2 min. The mica surface was rinsed immediately with nanopure water, and the surface was air-dried before being placed in the AFM for imaging. Images were acquired in air using a SNL (silicon tip on nitride lever) AFM probe (Agilent Technologies, force constant 21–98 N/m) and Agilent AFM controller operated in tapping mode. Imaging was

done at a resolution of 512  $\times$  512 pixels. Raw data were selected with the Picoimage software, and the same was used to “flatten” AFM images with second-order polynomial fitting. Each experiment was repeated four times.

**Single DNA Molecule Stretching Experiments.** Hop1 binding reactions were performed as described in the figure captions. In experiments involving zinc depletion, 1 mM EDTA was added to the assay buffer (20 mM Tris-HCl, pH 7.5, 50 mM NaCl, 1 mM EDTA). A modified transverse magnetic tweezers was used to achieve single DNA stretching. First,  $\lambda$ -DNA molecules (48 502 bp) were labeled at both ends with biotin-labeled oligonucleotides and then were flown into a glass channel and attached to a cover glass edge which had been coated with streptavidin. By subsequently flowing paramagnetic streptavidin-coated beads (Dynabeads M280 Streptavidin, Invitrogen, Singapore) into the channel and after incubation of 10 min, we obtained DNA tethers that were attached at one end to the glass coverslip edge and at the other to a paramagnetic bead. DNA extension was determined to be the difference between the centroid position of the bead and the edge of the cover glass along the force direction.

A pair of permanent magnets was used to generate force to the paramagnetic beads from 0.02 up to 50 pN in the focal plane. The forces were measured using the bead thermal motion:<sup>39,40</sup>  $f = k_B T z / \delta^2$ , where  $k_B$  is the Boltzmann constant,  $T$  the temperature,  $z$  the extension, and  $\delta^2$  the variance of the bead fluctuation in a direction perpendicular to the force.

To ensure we have a single DNA molecule between the bead and edge, assuming a persistence length of DNA is 50 nm, we computed its theoretical extension using the Marko-Siggia formula.<sup>21,23</sup> We then scanned for forces from 0.5 up to 10 pN. The persistence length of DNA was then measured in the force range by fitting the Marko-Siggia formula from the worm-like-chain DNA polymer model.<sup>21,23,39,40</sup> The DNA was determined to be a single DNA if the measured persistence length was in the range of 44–53 nm.

**DNA Circularization Assay.** Assay was performed as described previously.<sup>25,26</sup> Briefly, 0.5 nM <sup>32</sup>P-labeled 225 bp DNA fragment (derived from digestion of pUC19 plasmid DNA by digestion with *Ava*I) was incubated in the absence or presence of increasing concentrations of Hop1 in a 20  $\mu$ L reaction mixture containing 20 mM Tris-HCl, pH 7.5, and 0.1 mM ZnCl<sub>2</sub> as described above. After incubation at 30 °C for 30 min, we added 2.5 units of T4 DNA ligase (Fermentas, USA) and 1 $\times$  ligase buffer, and incubation was extended at 30 °C for 15 min. In experiments involving Exo III digestion, samples were further incubated at 37 °C for 20 min in the presence of 5 units of Exo III. The reactions were terminated by the addition of 1  $\mu$ L of 20% sodium dodecyl sulfate (SDS) and 1  $\mu$ L of 10 mg/mL proteinase K and incubated at 37 °C for 20 min. DNA was extracted with phenol–chloroform solution and precipitated with ethanol. DNA pellet was resuspended in 5  $\mu$ L of 6 $\times$  DNA gel loading buffer. Samples were subjected to electrophoresis through 8% polyacrylamide gel in 45 mM Tris–borate buffer (pH 8.3) containing 1 mM EDTA at 10 V/cm for 5 h. The dried gel was exposed to Fuji PhosphorImager screen, and the bands were visualized using software supplied by the manufacturer.

**Nuclease Protection Assays and Transformation Efficiency Assay.** A DNA fragment with a length of 600 bp from the 5'-end *HOP1* gene was amplified by polymerase chain reaction and purified using a Qiagen gel extraction kit (USA). In experiments with DNase I digestion, 450 ng of DNA fragment was incubated in a reaction mixture (20  $\mu$ L) containing 20 mM Tris-HCl, pH 7.5, 0.1 mM ZnCl<sub>2</sub>, 2 mM MgCl<sub>2</sub>, and 0.5 mM CaCl<sub>2</sub> in the absence or presence of increasing concentrations of Hop1 (0.5, 1, 1.5, 2, and 2.5  $\mu$ M). After incubation at 30 °C for 30 min, we added 0.05 U of DNase I (Fermentas), and incubation was extended at 37 °C for 4 min. Reaction was terminated by the addition of 1  $\mu$ L of 20% SDS and 1  $\mu$ L of 10 mg/mL proteinase K, followed by incubation at 37 °C for 15 min. Reaction mixtures were subjected to electrophoresis through 1.5% agarose gel and visualized by staining with ethidium bromide.

In experiments with *Bam*HI, Hop1 was incubated with a 600 bp DNA fragment as described above and then with *Bam*HI (6 U) containing 1 $\times$  reaction buffer. After incubation at 37 °C for 30 min, reaction was terminated by the addition of 1  $\mu$ L of 20% SDS and 1  $\mu$ L of 10 mg/mL proteinase K, followed by incubation at 37 °C for 15 min. Samples were subjected to electrophoresis through 1.5% agarose gel and visualized as described above.

In the transformation assay, linear pUC19 DNA (30 ng) was incubated in the absence or presence of increasing concentrations of Hop1 (150, 300, 450, and 550 nM) at 30 °C for 30 min and then with 1.5 U of T4 DNA ligase along with 1 $\times$  ligase reaction buffer. The protein was digested using 5  $\mu$ g of proteinase K at 37 °C for 15 min. The ligation mixture was then used for transformation of competent *E. coli* DH5 $\alpha$  cells, and the cells were spread on Luria–Bertani plates containing 50  $\mu$ g/mL ampicillin. The plates were incubated at 37 °C for 12 h. The colony-forming units were counted, and the values were plotted as bar graphs using Graph pad prism software.

**Conflict of Interest:** The authors declare no competing financial interest.

**Acknowledgment.** This work was supported by a grant (SR/SO/BB-94/2010) and J.C. Bose National Fellowship from the Department of Science and Technology, Government of India, New Delhi, to K.M. Work at Singapore was supported by the Mechanobiology Institute Singapore, to J.Y. We gratefully acknowledge Munia Ganguli for her assistance in the use of the atomic force microscope.

## REFERENCES AND NOTES

- Zickler, D.; Kleckner, N. Meiotic Chromosomes: Integrating Structure and Function. *Annu. Rev. Genet.* **1999**, *33*, 603–754.
- Zickler, D. From Early Homologue Recognition to Synaptonemal Complex Formation. *Chromosoma* **2006**, *115*, 158–174.
- Roeder, G. S. Meiotic Chromosomes: It Takes Two To Tango. *Genes Dev.* **1997**, *11*, 2600–2621.
- Paques, F.; Haber, J. E. Multiple Pathways of Recombination Induced by Double-Strand Breaks in *S. cerevisiae*. *Microbiol. Mol. Biol. Rev.* **1999**, *63*, 349–404.
- Hollingsworth, N. M.; Goetsch, L.; Byers, B. The *HOP1* Gene Encodes a Meiosis-Specific Component of Yeast Chromosomes. *Cell* **1990**, *61*, 73–84.
- Smith, A. V.; Roeder, G. S. The Yeast Red1 Protein Localizes to the Cores of Meiotic Chromosomes. *J. Cell Biol.* **1997**, *136*, 957–967.
- Sym, M.; Engebrecht, J.; Roeder, G. S. *ZIP1* Is a Synaptonemal Complex Protein Required for Meiotic Chromosome Synapsis. *Cell* **1993**, *72*, 365–378.
- Agarwal, S.; Roeder, G. S. Zip3 Provides a Link between Recombination Enzymes and Synaptonemal Complex Proteins. *Cell* **2000**, *102*, 245–255.
- Borner, G. V.; Kleckner, N.; Hunter, N. Crossover/Noncrossover, Differentiation, Synaptonemal Complex Formation and Regulatory Surveillance at the Leptotene/Zygotene Transition of Meiosis. *Cell* **2004**, *117*, 29–45.
- Fung, J. C.; Rockmill, B.; Odell, M.; Roeder, G. S. Imposition of Crossover Interference through the Nonrandom Distribution of Synapsis Initiation Complexes. *Cell* **2004**, *116*, 795–802.
- Klein, F.; Mahr, P.; Galova, M.; Buonomo, S. B.; Michaelis, C.; Nairz, K.; Nasmyth, K. A Central Role for Cohesins in Sister Chromatid Cohesion, Formation of Axial Elements, and Recombination during Yeast Meiosis. *Cell* **1999**, *98*, 91–103.
- Nag, D. K.; Scherthan, H.; Rockmill, B.; Bhargava, J.; Roeder, G. S. Heteroduplex DNA Formation and Homolog Pairing in Yeast Meiotic Mutants. *Genetics* **1995**, *141*, 75–86.
- Rockmill, B.; Roeder, G. S. Meiosis in Asynaptic Yeast. *Genetics* **1990**, *126*, 563–574.
- Loidl, J.; Klein, F.; Scherthan, H. Homologous Pairing Is Reduced but Not Abolished in Asynaptic Mutants of Yeast. *J. Cell Biol.* **1994**, *125*, 1191–1200.
- Caryl, A. P.; Armstrong, S. J.; Jones, G. H.; Franklin, F. C. A Homologue of the Yeast *HOP1* Gene Is Inactivated in the Arabidopsis Meiotic Mutant *asy1*. *Chromosoma* **2000**, *109*, 62–71.
- Zetka, M. C.; Kawasaki, I.; Strome, S.; Muller, F. Synapsis and Chiasma Formation in *C. elegans* Require HIM-3, a Meiotic Chromosome Core Component That Functions in Chromosome Segregation. *Genes Dev.* **1999**, *13*, 2258–2270.
- Yang, F.; De La Fuente, R.; Leu, N. A.; Baumann, C.; McLaughlin, K. J.; Wang, P. J. Mouse SYCP2 Is Required for SC Assembly and Chromosomal Synapsis during Male Meiosis. *J. Cell Biol.* **2006**, *173*, 497–507.
- Schwacha, A.; Kleckner, N. Identification of Joint Molecules That Form Frequently between Homologs but Rarely between Sister Chromatids during Yeast Meiosis. *Cell* **1994**, *76*, 51–63.
- Woltering, D.; Baumgartner, B.; Bagchi, S.; Larkin, B.; Loidl, J.; de los Santos, T.; Hollingsworth, N. M. Meiotic Segregation, Synapsis, and Recombination Checkpoint Functions Require Physical Interaction between the Chromosomal Proteins Red1p and Hop1p. *Mol. Cell. Biol.* **2000**, *20*, 6646–6658.
- Tripathi, P.; Anuradha, S.; Ghosal, G.; Muniyappa, K. Selective Binding of Meiosis-Specific Yeast Hop1 Protein to the Holliday Junctions Distorts the DNA Structure and Its Implications for Junction Migration and Resolution. *J. Mol. Biol.* **2006**, *364*, 599–611.
- Yan, J.; Marko, J. F. Effects of DNA-Distorting Proteins on DNA Elastic Response. *Phys. Rev. E* **2003**, *68*, 011905.



22. Liu, Y. J.; Chen, H.; Kenney, L. J.; Yan, J. A Divalent Switch Drives H-NS/DNA-Binding Conformations between Stiffening and Bridging Modes. *Genes Dev.* **2010**, *24*, 339–344.
23. Yan, J. Near-Field-Magnetic-Tweezer Manipulation of Single DNA Molecules. *Phys. Rev. E* **2004**, *70*, 011905.
24. Fu, W. B.; Wang, X. L.; Zhang, X. H.; Ran, S. Y.; Yan, J.; Li, M. Compaction Dynamics of Single DNA Molecules under Tension. *J. Am. Chem. Soc.* **2006**, *128*, 15040–15041.
25. Kironmai, K. M.; Muniyappa, K.; Friedman, D.; Hollingsworth, N.; Byers, B. DNA-Binding Activities of Hop1 Protein, a Synaptonemal Complex Component from *S. cerevisiae*. *Mol. Cell. Biol.* **1998**, *18*, 1424–1435.
26. Shore, D.; Langowski, J.; Baldwin, R. L. DNA Flexibility Studied by Covalent Closure of Short Fragments into Circles. *Proc. Natl. Acad. Sci. U.S.A.* **1981**, *78*, 4833–4837.
27. McClintock, B. The Association of Non-homologous Parts of Chromosomes in the Mid-prophase of Meiosis in *Zea mays*. *Z. Zellforsch. Mikrosk. Anat.* **1933**, *19*, 191–237.
28. Page, S. L.; Hawley, R. S. The Genetics and Molecular Biology of the Synaptonemal Complex. *Annu. Rev. Cell Dev. Biol.* **2004**, *20*, 525–558.
29. Heyer, W. D.; Ehmsen, K. T.; Liu, J. Regulation of Homologous Recombination in Eukaryotes. *Annu. Rev. Genet.* **2010**, *44*, 113–39.
30. Kornysheva, A. A.; Wynveen, A. The Homology Recognition Well as an Innate Property of DNA Structure. *Proc. Natl. Acad. Sci. U.S.A.* **2009**, *106*, 4683–4688.
31. Anuradha, S.; Muniyappa, K. *Saccharomyces cerevisiae* Hop1 Zinc Finger Motif Is the Minimal Region Required for Its Function *in Vitro*. *J. Biol. Chem.* **2004**, *279*, 28961–28969.
32. Anuradha, S.; Muniyappa, K. Meiosis-Specific Yeast Hop1 Protein Promotes Synapsis of Double-Stranded DNA Helices via the Formation of Guanine Quartets. *Nucleic Acids Res.* **2004**, *32*, 2378–2385.
33. Blat, Y.; Protacio, R. U.; Hunter, N.; Kleckner, N. Physical and Functional Interactions among Basic Chromosome Organizational Features Govern Early Steps of Meiotic Chiasma Formation. *Cell* **2002**, *111*, 791–802.
34. Panizza, S.; Mendoza, M. A.; Berlinger, M.; Huang, L.; Nicolas, A.; Shirahige, K.; Klein, F. Spo11-Accessory Proteins Link Double-Strand Break Sites to the Chromosome Axis in Early Meiotic Recombination. *Cell* **2011**, *146*, 372–383.
35. Kleckner, N.; Weiner, B. M. Potential Advantages of Unstable Interactions for Pairing of Chromosomes in Meiotic, Somatic and Premeiotic Cells. *Cold Spring Harbor Symp. Quant. Biol.* **1993**, *58*, 553–565.
36. Danilowicz, C.; Lee, C. H.; Kim, K.; Hatch, K.; Coljee, V. W.; Kleckner, N.; Prentiss, M. Single Molecule Detection of Direct, Homologous, DNA/DNA Pairing. *Proc. Natl. Acad. Sci. U.S.A.* **2009**, *106*, 19824–19829.
37. Tsubouchi, T.; Roeder, G. S. A Synaptonemal Complex Protein Promotes Homology-Independent Centromere Coupling. *Science* **2005**, *308*, 870–873.
38. Khan, K.; Madhavan, T. P. V.; Muniyappa, K. Cloning, Overexpression and Purification of Functionally Active *S. cerevisiae* Hop1 Protein from *E. coli*. *Protein Expression Purif.* **2010**, *72*, 42–50.
39. Strick, T. R.; Allemand, J. F.; Bensimon, D.; Bensimon, A.; Croquette, V. The Elasticity of a Single Supercoiled DNA Molecule. *Science* **1996**, *271*, 1835–1837.
40. Skoko, D.; Yan, J.; Johnson, R. C.; Marko, J. F. Low-Force DNA Condensation and Discontinuous High-Force Decondensation Reveal a Loop-Stabilizing Function of the Protein Fis. *Phys. Rev. Lett.* **2005**, *95*, 208101.